HHS Public Access

Author manuscript

Acta Biomater. Author manuscript; available in PMC 2020 December 01.

Published in final edited form as:

Acta Biomater. 2019 December ; 100: 105–117. doi:10.1016/j.actbio.2019.09.043.

Inflammation via myeloid differentiation primary response gene 88 (MyD88) signaling mediates the fibrotic response to implantable synthetic poly(ethylene glycol) hydrogels

Luke D. Amer[a,b,1], **Leila S. Saleh**[a,1], **Cierra Walker**[b,c], **Stacey Thomas**[d], **William J. Janssen**[d,e], **Scott Alper**[f,g], **Stephanie J. Bryant**[a,b,c,2]

[a]Department of Chemical and Biological Engineering, University of Colorado, Boulder, CO 80309;

[b]BioFrontiers Institute, University of Colorado, Boulder, CO 80309;

[c]Material Science and Engineering Program, University of Colorado, Boulder, CO 80309;

[d]Division of Pulmonary, Sleep and Critical Care Medicine, National Jewish Health, Denver, CO 80206

[e]Division of Pulmonary Sciences and Critical Care Medicine, University of Colorado Denver, Aurora, CO 80045;

[f]Department of Biomedical Research and Center for Genes, Environment and Health, National Jewish Health, Denver, CO 80206;

[g]Department of Immunology and Microbiology, University of Colorado School of Medicine, Aurora, CO 80045

Abstract

Synthetic hydrogels, such as poly(ethylene glycol) (PEG), are promising for a range of *in vivo* applications. However, like all non-biological biomaterials, synthetic hydrogels including PEG elicit a foreign body response (FBR). The FBR is thought to be initiated by adsorbed protein that is recognized by and subsequently activates inflammatory cells, notably macrophages, and culminates with fibrotic encapsulation. However, the molecular mechanisms that drive the FBR are not well understood. Toll-like receptors (TLRs) are key receptors that recognize pathogens, but also recognize altered host proteins that display damage-associated molecular patterns (DAMPs). Thus TLRs may play a role in the FBR. Here, we investigated myeloid differentiation primary response gene 88 (MyD88), a signaling adaptor protein that mediates inflammatory cytokine production induced by most TLRs. An *in vitro* model was used consisting of macrophages

[2]To Whom Correspondence Should be addressed. stephanie.bryant@colorado.edu.
[1]LDA and LSS contributed equally to this work

Declaration of conflict of interest
None.

Data Availability
Data will be made available upon request.

cultured on the surface of synthetic hydrogels, specifically PEG, with pre-adsorbed serum proteins. Our *in vitro* findings demonstrate that MyD88-dependent signaling is the predominant inflammatory pathway in macrophage activation to synthetic hydrogels. When stimulated with TLR agonists to mimic additional DAMPs present *in vivo*, MyD88-dependent signaling was also the predominant pathway in macrophage activation. An *in vivo* model of PEG hydrogels implanted subcutaneously in wild-type and MyD88$^{-/-}$ mice also demonstrated that MyD88 is the key contributor to the recruitment of inflammatory cells and formation of the fibrous capsule surrounding the implanted hydrogel. Taken together, findings from this study identify MyD88-mediated inflammation as being a critical pathway involved not only in the inflammatory response, but in formation of the fibrous capsule to PEG hydrogels.

Graphical Abstract

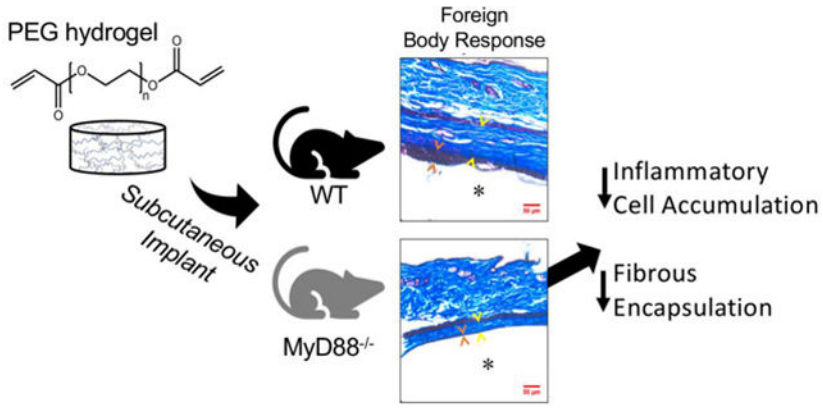

Keywords

Foreign Body Response; macrophage; PEG hydrogel; MyD88; fibrous encapsulation

1. Introduction

Synthetic hydrogels are promising in a range of implantable devices including hydrophilic coatings applied to permanent medical devices, drug depots for controlled release and tissue engineering [1]. In particular, poly(ethylene glycol) (PEG) hydrogels are being investigated as coatings for implants [2–4] and as cell carriers for tissue engineering due to their ease with which to tune their properties and incorporate biological functionality to direct cell fate and function and/or delivery molecules [5–8]. However, as with all non-biological materials, the innate immune system recognizes these materials as foreign. This leads to a cascade of events that make up the foreign body response (FBR) [9,10]. While many implanted devices function despite a FBR (e.g., artificial joints), the FBR has limited the advancement of new implantable devices (e.g., glucose sensors) [11] and has hampered tissue engineering when synthetic hydrogels are employed *in vivo* [12,13]. Although its severity depends on material chemistry, mechanics, and topography [9], the FBR occurs to all non-biological implanted materials, including implanted PEG hydrogels [14,15]. However, the mechanisms underlying this response remain to be elucidated.

The hallmark of the FBR is formation of an avascular fibrous capsule that walls off the implant from the host and limits communication with the surrounding tissue [9,16]. Macrophages have long been considered key orchestrators of the FBR [17,18]. However, how they interact with the implant and how these interactions influence their programming remains unknown. Moreover, the role of inflammation in mediating the fibrotic response has yet to be established. Since encapsulation hampers integration of implanted materials into the host tissue, understanding the role of inflammatory pathways in fibrosis may be critical to implant success.

Toll-like receptors (TLRs) are conserved membrane receptors that recognize pathogens and subsequently activate innate immune cells [19]. TLR2 and TLR4 also recognize endogenous molecules known as damage-associated molecular patterns or DAMPs [20,21]. DAMPs can arise from tissue damage induced by biomaterial implantation. For example, we identified over two hundred proteins adsorbed to the surface of implanted poly(ethylene glycol) (PEG) hydrogels [22]. A subset of these identified proteins signal through TLR2, TLR4, or both [23] and include components of the extracellular matrix (e.g., fibronectin and fibrinogen) and cells (e.g., heat shock proteins such as HSP70 and high-mobility group box 1) [24–27]. Endogenous proteins that unfold at a biomaterial surface may also signal as DAMPs [28–32]. Not all molecules that adsorb to an implant surface lead to the FBR [33], but rather, those that act as DAMPs may facilitate the FBR [34]. Moreover, protein interaction with surfaces is highly dynamic [28]. This leads to adsorption and desorption processes where macrophages can interact with proteins throughout the adsorbed protein layer. Several studies investigated the FBR in mice deficient in TLR4. At the early stages (i.e., 14 d) of fibrous encapsulation, one study reported no dependence on TLR4 [35], while another study showed that if fibrinogen was pre-adsorbed to the implant prior to implantation to exacerbate the FBR, a partial reduction in fibrous encapsulation was observed in TLR4 deficient mice [36]. These *in vivo* studies suggest that DAMPs acting through pre-adsorbed proteins mediate fibrous encapsulation and that the level of DAMPs contribute to the temporal response.

Inflammatory cytokine production induced by stimulation of most TLRs is mediated by the adaptor protein myeloid differentiation primary response gene 88 (MyD88). The sole exceptions are TLR3, which is mediated by a second signaling adaptor TRIF, and TLR4, which is mediated by both MyD88 and TRIF. The MyD88 signaling adaptor also mediates IL-1 inflammatory responses, including IL-1β, which is a key inflammatory cytokine. Thus, MyD88 is considered a central signaling molecule that mediates inflammation [37]. MyD88-dependent inflammation occurs through NF-κB mediated transcription of pro-inflammatory cytokines [19]. The TRIF-dependent pathway also up-regulates NF-κB activity, although not to the same extent [19]. Mice deficient in MyD88 have greatly diminished inflammatory responses induced by multiple TLRs and cytokine signals [38–40]. In the context of the FBR, studies reported that MyD88 contributes to osteolysis induced by poly(methyl methacrylate) wear particles *in vivo* [41], and contributes to the inflammatory response of dendritic cells to biomaterials *in vitro* [42]. MyD88 has also been shown to induce NF-κB activation in macrophages *in vitro* in response to unpurified alginate containing pathogen-associated molecular patterns [43]. These studies indicate that MyD88 is an important mediator of the inflammatory response not only to pathogens but also to sterile biomaterials.

However, a key question remains as to whether sterile inflammation associated with biomaterial implantation drives the fibrotic response in the FBR.

Targeting MyD88 offers the opportunity to affect nearly all TLRs and thus we chose to investigate MyD88 for its role in the FBR to PEG hydrogel implants (Fig. 1A). We first investigated inflammatory responses of macrophages that were derived from wild-type (WT) and MyD88$^{-/-}$ mice and cultured on PEG hydrogels. Since the FBR is thought to be initiated by adsorbed proteins that are recognized by macrophages, hydrogels were pre-exposed to serum. We next introduced a TLR4 agonist to simulate the presence of DAMPs in the *in vivo* milieu, but which would not be present in serum. To delineate the contribution of MyD88-independent signaling during TLR4 activation, an agonist for TLR3 was investigated. Finally, the PEG hydrogels were implanted subcutaneously in WT and MyD88$^{-/-}$ mice to study the role of MyD88-mediated inflammation in immune cell recruitment and fibrous encapsulation. The experimental design for this study is shown in Fig. 1B. Findings from this study shed new light on the role of inflammation in regulating fibrous encapsulation to PEG hydrogels. Given the ubiquitous nature of the FBR, this information is expected to aid in identifying effective strategies that more broadly control and abrogate fibrous encapsulation to implanted materials by targeting inflammation.

2. Materials and methods

2.1. Hydrogel formation

Poly(ethylene glycol) (PEG) diacrylate macromolecular monomers were synthesized by reacting PEG (MW 3000, Sigma) with 8M excess acryloyl chloride with trimethylamine in toluene under nitrogen, in the dark, overnight. The product was recovered by filtration over aluminum oxide, precipitation. Greater than 90% of the hydroxyls of each PEG molecule were functionalized with acrylates by ^{1}H NMR (Fig. S1). Hydrogels were formed from a sterile-filtered (0.22 μm) solution of 20% (w/w) PEG-dA and 0.05% (w/w) photoinitiator (Irgacure 2959, BASF) in phosphate buffered saline (PBS) at 352 nm light and ~6 mW/cm^2 for 10 minutes. Cylindrical hydrogels of 0.8 mm height and 6 mm diameter were used *in vitro* and of 2 mm height and 4.5 mm diameter were used *in vivo*. All procedures were performed using aseptic techniques. Hydrogels were swollen to equilibrium in sterile PBS prior to performing any experiments.

2.2 Hydrogel characterization

PEG hydrogels were allowed to equilibrate in PBS for 36 hours prior to testing. The compressive modulus was determined by compression to 15% strain at 0.5mm/min on an MTS Synergie 100 with a 10N load cell. The compressive modulus was determined by the slope of the linear region between 10 and 15% strain on the stress-strain curve. The hydrogels were weighed (wet weight, m_w) then lyophilized to obtain the polymer dry weight (m_d). The equilibrium mass swelling ratio was determined by $m_{w/}m_d$.

2.3. In Vitro Assessment of Protein Adsorption

Equilibrium swollen PEG hydrogels 6mm in diameter were placed in 96-well tissue culture polystyrene (TCPS) plates. Hydrogels and 96-well TCPS plates without hydrogel, which is

referred to as the reference substrate, were exposed to 100% fetal bovine serum (FBS) for 2 hours, consistent with our previously established protocols [44,45]. The FBS then was aspirated. Hydrogels were placed in 5% (w/v) sodium dodecyl sulfate (SDS) solution and SDS solution was added directly to the wells in TCPS reference substrate. After two hours, the solution was collected, flash frozen in liquid nitrogen, and stored at −70°C. Total protein mass quantified (bicinchoninic acid, BCA assay, Pierce) was normalized to exposed surface area. Protein (4 μg/lane, n=4) was loaded onto a 4–20% tris glycine polyacrylamide gel (BioRad). Protein bands were imaged by silver staining (Pierce) and a VersaDoc MP 4000 Imager (BioRad).

2.4. Primary macrophage isolation and treatment

Primary bone marrow derived macrophages were obtained [46] from bone marrow aspirate collected from femurs and tibiae of 7 week old C57BL/6 mice (Charles River Laboratories) or B6.129P2(SJL)-MyD88<tm1.1Defr>/J mice (Jackson Laboratories) and placed in medium containing Iscove's Modified Dulbecco's Medium (IMDM), 20% FBS, 100 U/ml penicillin, 100 U/ml streptomycin and 2.5 μg/ml fungizone (PSF) and layered in Lympholyte M (Accurate Chemicals). Mononuclear cells were plated on non-TCPS and differentiated into macrophages in IMDM, 20% FBS, 2 mL-glutamine, in PSF, 1.5 ng/ml human macrophage colony stimulating factor (R&D systems) and 100 ng/ml human FLT-3 (R&D systems) for 10 days. Hydrogels and the reference substrate, TCPS, were exposed to FBS for two hours at room temperature to allow proteins to adsorb; the FBS was then removed by aspiration. Macrophages were seeded on the surface of equilibrium swollen PEG hydrogels or on the reference substrate with pre-adsorbed serum proteins at 2,650 macrophages/mm^2 under: (a) no treatment, (b) 10 ng/ml lipopolysaccharide (LPS, Sigma), or (c) 1 μg/ml poly(I:C) (InvivoGen) in medium containing IMDM, 20% FBS, and PSF.

2.5. In vitro assessment of macrophage activation

After treatment for four hours, cells were lysed in TRK lysis buffer (Omega Biotek) containing β-mercaptoethanol (Sigma) and RNA isolated (E.Z.N.A.® RNA Isolation Kit, Omega Biotek). Equal amounts of RNA were reverse transcribed into cDNA (High-Capacity cDNA Reverse Transcription Kit, Thermo Scientific). Quantitative PCR was performed on a CFX96™ Real-Time PCR Detection System (Biorad) with Fast SYBR Green Master Mix (Roche). Custom primers were validated and efficiencies [47] listed in Table 1. Data are presented as expression relative to the housekeeping gene *Rpl32* calculated by $E_{HKG}^{CT_{HKG}}/E_{GOI}^{CT_{GOI}}$ [47]. Fold-change calculated by $(RE_{hydrogel} - RE_{ref})/RE_{ref}$; *ref* is the reference substrate. CT values for *Rpl32* were consistent across all samples in macrophages from WT and MyD88$^{-/-}$ mice. After treatment for 24 hours, media were collected and assessed for the cytokines tumor necrosis factor alpha (TNF-α) and interleukin-6 (IL-6) by standard enzyme-linked immunosorbent assay kits (ELISA, R&D Systems).

2.6. Hydrogel implantation

Equilibrium swollen PEG hydrogel disks were implanted into dorsal subcutaneous pockets of 7-week old male C57BL/6 mice (Charles River Laboratories) or B6.129P2(SJL)-MyD88<tm1.1Defr>/J mice (Jackson Laboratories) for 2, 7, and 28 days. Four hydrogels

were implanted per mouse, one over each shoulder and one over each hip, and incisions were closed with surgical staples. Prior to implantation, hydrogels were confirmed endotoxin-free (Limulus Amebocyte Lysate test kit, GenScript). Mice were euthanized via CO_2 inhalation and subsequent cervical dislocation. Two hydrogels were lost post-implantation in one WT mice at day 28. All animal protocols were approved by the University of Colorado at Boulder Institutional Animal Care and Use Committee (IACUC) and follow the NIH guidelines for animal care.

2.7. In vivo assessment and analysis

To monitor cell attachment to implanted hydrogels, hydrogels were explanted at 2 days and removed from the surrounding tissue. Hydrogel were fixed in 10% neutral buffered formalin for 30 minutes at room temperature, treated with Alexfluor 488 Phalloidin (1:30) for 30 minutes, counterstained with DAPI, and imaged by laser scanning confocal microscopy (Zeiss LSM5 Pascal).

To determine leukocyte types surrounding the implants, flow cytometry was performed. Hydrogels and the surrounding tissue were explanted at 2, 7, and 28 days. To obtain a sufficient number of cells, four hydrogels were pooled. Tissue and hydrogels were explanted and immediately minced and digested with liberase TM (Roche) for 30 minutes at 37°C; tissue digestion was then stopped with 10 mM ethylenediaminetetraacetic acid (EDTA, Bio-Rad) in Roswell Park Memorial Institute Medium (RPMI, Corning). Cells were filtered (100 μm cell strainer) and fixed with 4% paraformaldehyde for 15 minutes on ice. Freshly isolated cells were stained for 30 min with the following conjugated anti-mouse monoclonal antibodies: Purified CD16/CD32 (Clone 93, eBioscience 14-0161-85), FITC CD45 (Clone 30-F11, BD Biosciences 5503080), PE-Cy7 CD3e (Clone 145–2C11, eBioscience 25-0031-81), APC-Cy7 CD19 (Clone eBio1D3, eBioscience 47-0193-82), BUV395 CD11b (Clone M1/70, BD Biosciences 563553), PE Siglec-F (Clone E50–2440, BD Biosciences 552126), Pacific Blue Ly-6G (Clone 1A8, Biolegend 127612), PerCP-Cy5.5 Ly-6C (Clone HK1.4, eBioscience 45-5932-82), and Alexa Fluor 647 CD64 (Clone X54–5/7.1, BD Biosciences 558539). Analysis was conducted using the LSR II (BD Biosciences) flow cytometer and FlowJo (Tree Star) software to identify leukocyte populations. Leukocyte populations were first identified as $CD45^+$. CD3e and CD19 double negative cells were used in subsequent analyses to identify myeloid populations. Eosinophils were identified by their double positive Siglec-F and CD11b profile. Neutrophils ($Ly\text{-}6G^+$, $Siglec\text{-}F^-$, Low SSC), monocytes ($CD64^{lo\text{-}hi}$ $Ly\text{-}6G^-$, $Ly\text{-}6C^+$, $Siglec\text{-}F^-$, Low SSC) and macrophages ($CD64^{lo\text{-}hi}$, $Ly\text{-}6G^-$, $Ly\text{-}6C^-$) were identified.

To monitor the FBR, a set of hydrogels and surrounding tissue was explanted at 2, 7, and 28 days after implantation and fixed in 10% buffered formalin for 4 hours at room temperature. Following dehydration and embedding in paraffin wax, samples were sectioned into 10 μm thick slices, and stained with Masson's Trichrome that uses hematoxylin as a nuclear counterstain. Samples were imaged with brightfield microscopy (Axiovert 40C Zeiss). The thickness of inflammatory cells at the surface of the hydrogels was quantified (NIH ImageJ) by the distance of the layer of purple nuclei from the hydrogel surface to the collagenous

layer. At day 28, the fibrous capsule thickness was measured as the distance from the end of the inflammatory cell layer to the subdermal muscle layer.

2.8. Statistical Analysis

In vitro: data are presented as mean (n=6 for hydrogel properties and n=4 for the gene expression and ELISA data) with standard deviation as error bars or reported parenthetically in the text. *In vivo*: For flow cytometry analysis, four hydrogels from one mouse per strain per time point were pooled together to obtain sufficient cell numbers for analysis. These results therefore demonstrate trends in the relative percentage of cell types as statistical significance was not obtained. For histology, data are the mean of n =8 hydrogels from two WT mice or n=4 hydrogels from one MyD88$^{-/-}$ mouse for day 2 and 7, and the mean of n = 6 hydrogels from two WT mice and the mean of n=8 hydrogels from two MyD88 mice for day 28. Quantification of histology was taken from four measurements at random per hydrogel sample and averaged for the inflammatory cell thickness and fibrous capsule thickness. Data are shown as the mean of individual hydrogels with standard deviation as error bars or reported parenthetically in the text. The relative variability among hydrogels for a given animal and between animals was similar. For example the coefficient of variance for the fibrous capsule measurement was 10% between animals and 11% within an animal. Statistical analysis was performed with Real Statistics and Excel by two-way or three-way ANOVAs followed by Tukey's HSD (α=0.05). If three-way interactions were statistically significant, follow-up analyses were performed for simple two-way interactions and main effects. Statistical significance was set at $p<0.05$.

3. Results

3.1. Macrophage activation by synthetic hydrogels in vitro is mediated by MyD88 signaling

Synthetic PEG hydrogels were investigated due to their promise in drug delivery, cell encapsulation and tissue engineering. Tissue culture polystyrene (TCPS) was used as a reference substrate. PEG hydrogels were formed with 20% PEGdA resulting in a compressive modulus of 164 kPa and an equilibrium swelling ratio of 9.2 (Fig. 2A). An *in vitro* model was used where serum proteins from fetal bovine serum were pre-adsorbed to the hydrogel and to the reference substrate to mimic the initial *in vivo* events of the FBR. The amount of pre-adsorbed protein was ~2.5-fold higher on PEG hydrogels when compared to the reference substrate (Fig. 2B). The protein signature, however, was similar, with the majority of proteins being larger than 50 kDa (Fig. 2C). Due to the tight mesh of the hydrogel, these proteins will be restricted to the hydrogel surface [48].

Bone marrow-derived macrophages were differentiated from mononuclear cell isolates obtained from WT and MyD88$^{-/-}$ mice. Macrophages were seeded on top of PEG hydrogels and onto the reference substrate TCPS, with pre-adsorbed serum proteins, which could act as DAMPs (Fig. 3A). After 4 h, macrophage activation was assessed by quantitative RT-PCR for expression of tumor necrosis factor-α (*Tnfa*), interleukin-6 (*Il6*), and interleukin-1β (*Il1b*), which are all regulated by NF-κB. Macrophage interrogation of the hydrogel led to significant increases in expression of all three genes (Fig. 3B). In MyD88$^{-/-}$ macrophages,

expression levels of the pro-inflammatory cytokines were reduced to baseline levels of WT macrophages on the reference substrate. The difference in cytokine expression levels in MyD88$^{-/-}$ from WT macrophages on the reference substrate was not statistically significant. Accumulation of TNF-α and IL-6 in the culture medium after 24 h was below the sensitivity of the ELISA (≤~8 pg/ml), which may be attributed to the absence of strong DAMPs in serum. Overall, these results indicate a hydrogel-induced inflammatory response that is dependent on MyD88 and suggests that adsorbed proteins and/or the underlying substrate chemistry induce macrophage activation in a manner that was not observed with the reference substrate.

3.2. Macrophage activation to synthetic hydrogels in the presence of a DAMP-mimetic is largely mediated by MyD88 signaling in vitro

The inflammatory response that is induced as part of the FBR by implanted materials *in vivo* is a sterile response and is thought to be mediated by DAMPs present in the post-implantation microenvironment. We therefore next used our *in vitro* model to assess macrophage activation in the presence of the hydrogel, pre-adsorbed serum proteins, and a DAMP-mimetic. Since many DAMPs bind to TLRs, we chose lipopolysaccharide (LPS), a TLR4 agonist, as the DAMP-mimetic. LPS induces a response mediated by a MyD88-dependent and a MyD88-independent pathway, both of which initiate NF-κB transcriptional upregulation of pro-inflammatory cytokines (Fig. 4A) [19].

Using the *in vitro* model in Fig. 1B co-stimulated with LPS, macrophage pro-inflammatory responses were assessed at the mRNA and protein levels. LPS was added to the culture medium at the time of macrophage seeding. With LPS stimulation, mRNA levels of the pro-inflammatory cytokines *Tnfa*, *Il6*, and *Il1b* increased significantly after 4 h for the reference substrate and the hydrogel (Fig. 4B). Moreover, *Tnfa* expression was significantly higher for the hydrogel and LPS than when exposed to either hydrogel or LPS alone (Fig. 4B). Among all three genes, the fold-change in mRNA levels due to the hydrogel was more pronounced in the absence of LPS (i.e., 4–11-fold) when compared to LPS stimulation (i.e., ≤2-fold) (Fig. 4C). MyD88$^{-/-}$ macrophages had significantly reduced pro-inflammatory cytokine expression compared to WT macrophages after 4 h on the hydrogel and the reference substrate under LPS stimulation (Fig. 4B). The fold-change in mRNA levels due to the hydrogel in MyD88$^{-/-}$ macrophages was lower than in WT macrophages without LPS, but was not affected under LPS stimulation (Fig. 4C). Lastly, approximately 300 pg/ml TNF-α and 850–900 pg/ml IL-6 had accumulated after 24 h with LPS stimulation, but there was no significant difference with the hydrogel (Fig. 4D). There was significantly less TNF-α and IL-6 in the medium with MyD88$^{-/-}$ macrophages. These results indicate that the hydrogel contributes to the overall macrophage response, although to a lesser extent in the presence of a strong DAMP-mimetic, and that the overall response is largely through MyD88-dependent signaling.

3.3. Macrophage activation to synthetic hydrogels in the presence of an agonist for MyD88-independent signaling is partially mediated by MyD88 signaling in vitro.

The response to the DAMP-mimetic (*i.e.*, LPS), the hydrogel, and the combination is largely dependent on MyD88 signaling (Fig. 3,4). To better delineate the interaction between the

hydrogel and MyD88-dependent signaling in response to TLR4 activation, we exposed macrophages to a combination of hydrogel and poly(I:C). Poly(I:C) is sensed by TLR3, which activates the MyD88-independent TRIF pathway that can also induce NF-κB-mediated transcription of pro-inflammatory cytokines (Fig. 5A) [19]. Poly(I:C) was added to the culture medium at the time of seeding using the same *in vitro* model outlined in Fig. 1B.

With poly(I:C) stimulation, mRNA expression of all three genes was significantly higher when compared to the unstimulated condition; likewise, mRNA levels for these three cytokines were increased in the presence of the hydrogel compared to the reference substrate (Fig. 5B). The mRNA production, however, was lower when compared to the LPS stimulated condition for the hydrogel and the reference substrate (compare Fig. 5B to Fig. 4B). For example, *Tnfa* expression was 3.5-fold lower while *Il1b* expression was 21.6-fold lower on the hydrogel with poly(I:C) compared to LPS. The contribution of the hydrogel was more evident under poly(I:C) stimulation (i.e., 3–4-fold) than LPS stimulation (i.e., ≤2-fold) (compare Fig. 5C to Fig. 4C). In MyD88$^{-/-}$ macrophages that were stimulated with poly(I:C), the production of cytokine mRNA was reduced, but the levels were still higher than in unstimulated MyD88$^{-/-}$ macrophages (Fig. 5B). Moreover, expression for all three genes was significantly higher in MyD88$^{-/-}$ macrophages on the hydrogel compared to the reference substrate under poly(I:C) stimulation (Fig. 5B). The fold-change in mRNA levels due to the hydrogel under poly(I:C) stimulation was reduced in MyD88$^{-/-}$ macrophages compared to WT macrophages for *Il1b* expression, which is contrary to LPS stimulation where no difference was observed. However, the fold-change due to the hydrogel was not different between MyD88$^{-/-}$ and WT macrophages for *Tnfa* and *Il6* expression; a finding similar to LPS simulation. Lastly, approximately 50–70 pg/ml TNF-α and 40–50 pg/ml IL-6 had accumulated in the cultures after 24 h with poly(I:C) stimulation, but there was no significant difference due to the hydrogel (Fig. 5D). In MyD88$^{-/-}$ macrophages, TNF-α and IL-6 protein levels were strongly diminished. Contrary to LPS, these findings demonstrate that the hydrogel had a significant contribution to the mRNA production of pro-inflammatory cytokines in macrophages under poly(I:C) activation. Moreover, these results show that MyD88 partly mediates macrophage activation under poly(I:C) stimulation on the reference substrate and to a greater extent on the hydrogel. Because the initial response to poly(I:C) is MyD88-independent, this suggests a feedback mechanism, possibly involving IL-1β production that stimulates MyD88-dependent signaling, but also suggests that the hydrogel and/or its adsorbed proteins may be contributing to the MyD88-dependent signaling.

3.4. Inflammatory cell accumulation and fibrous capsule formation in response to implanted synthetic hydrogels are diminished in MyD88$^{-/-}$ Mice.

To investigate the effects of MyD88 on the FBR *in vivo*, hydrogels were implanted in subcutaneous pockets of WT and MyD88$^{-/-}$ mice (Fig. 6A). We first investigated the infiltration of cells to the implant site, where recruitment of inflammatory cells occurs in the initial stages of the FBR. Within 2 d post-implantation, cells had infiltrated to the implant and attached to the hydrogel surface (Fig. 6B). This occurred without any adhesion moieties incorporated into the hydrogels. Fewer cells were attached to the hydrogel surface in MyD88$^{-/-}$ mice (Fig. 6B). To identify the types of inflammatory cells that accumulated at

the implant site, hydrogels and the tissue immediately surrounding them were removed, enzymatically digested, and assessed with flow cytometry (Fig. 6C, D). In WT mice, almost half of the leukocytes were neutrophils (Fig. 4E). The remainder was comprised of macrophages, monocytes, and eosinophils. Lymphocytes (assessed with CD3 and CD19) were not detected (data not shown). In comparison, in MyD88$^{-/-}$ mice the relative frequency of neutrophils trended lower (<20%), and the majority of leukocytes were macrophages and monocytes. It is important to note that because the samples analyzed by flow cytometry were pooled to achieve sufficient numbers of cells, the results are intended to indicate the cell types present and are limited to trends in the relative frequency of the cell types. This finding is concomitant with an overall lower number of inflammatory cells in the MyD88$^{-/-}$ mice as shown in Fig. 7.

As a next step, the kinetics of inflammatory cell infiltration and fibrous capsule formation were evaluated (Fig. 7A). Explants were assessed histologically 2, 7, and 28 d post-implantation for inflammatory cells and fibrous encapsulation (Fig. 7B). The layer of inflammatory cells was quantified by measuring the distance between implant and dermis (Fig. 7C). In WT mice, a characteristic inflammatory response was observed, with several layers of inflammatory cells at the hydrogel surface as early as 2 d and persisting to 28 d. The thickness of the inflammatory cell layer was lower in MyD88$^{-/-}$ mice across all time points; for example decreasing 5.5-fold from 50 (20) μm in WT to 6 (4) μm in MyD88$^{-/-}$ mice at 2 d. To identify the kinetics of inflammatory cells accumulating around the implants, flow cytometry was again performed using the gating strategy outlined in Fig. 4. The following trends were observed. In WT mice, neutrophils continued to be highly abundant through to 28 d (Fig. 5D). Macrophages accounted for almost half of the peri-implant leukocytes at 2 d. On day 7 and 28, macrophages were relatively less frequent than on 2 d. However, the thickness of the inflammatory cell layer increased at these time points. Hence, the total number of macrophages may not have changed substantially. Lastly, there was a detectable influx of monocytes into the inflammatory layer in WT mice. In MyD88$^{-/-}$ mice, macrophages accounted for over half of the inflammatory cells surrounding the implant at all time points; although the total number of inflammatory cells was far lower. Neutrophils and monocytes were less frequent. A collagenous fibrous capsule was evident surrounding the hydrogels in WT mice with an average thickness of 90 μm (Fig. 7B and 7E). There was evidence of vascularization in the fibrous capsule in WT mice (Fig. 7B). In MyD88$^{-/-}$ mice, the fibrous capsule was significantly reduced by 3-fold. The capsule remained dense with vascularization less apparent, which is attributed to the thinner capsule. Taken as a whole, these data suggest that recruitment of inflammatory cells to the implant is markedly impaired in MyD88$^{-/-}$ mice. This corresponds to reduced fibrous capsule formation.

4. Discussion

The FBR to implanted biomaterials is a complex process involving many cell types, with macrophages implicated as the primary orchestrator [10,49]. However, the signaling pathways regulating macrophage function in the context of the FBR are not well understood. Findings from this study demonstrate that the adaptor protein MyD88, which is a central mediator of inflammation and leads to NF-κB activation, is required for the FBR to PEG hydrogels. The *in vitro* studies show that MyD88-dependent pathways are the dominant

mechanisms that lead to inflammatory responses in macrophages induced by PEG hydrogels. The *in vivo* studies show that MyD88 is involved in inflammatory cell recruitment to the surface of implanted PEG hydrogels and contributes significantly to fibrous encapsulation. Taken together, findings from this work demonstrate that inflammation mediated by MyD88 plays a significant role in the fibrotic response of the FBR to implanted PEG hydrogels.

Macrophages are highly sensitive to the substrate to which they are attached, affecting how they respond to DAMPs in the surrounding milieu. Our *in vitro* data demonstrate that the PEG hydrogel when compared to the reference substrate of TCPS induced a MyD88-dependent inflammatory response in macrophages that contributed to the overall inflammatory response in the presence of a soluble DAMP-mimetic. Macrophages interact with the hydrogel through pre-adsorbed proteins and/or the underlying material surface. Although the signature of the adsorbed proteins on the hydrogel was similar to the reference substrate, there were differences. The higher amount of adsorbed protein on PEG hydrogels can be attributed to the nature by which water interacts and entraps proteins at hydrophilic and neutral surfaces [50]. While proteins may diffuse into the hydrogel due to its crosslinked network, the recovered adsorbed serum proteins were ~50 kDa or larger and therefore are expected to be restricted to the surface of the hydrogel. Studies have reported that bovine serum albumin, the most abundant protein in serum with a molecular weight of 67 kDa [51], does not readily diffuse into PEG hydrogels of similar or more loosely crosslinked hydrogels [48]. Although smaller proteins that were not detectable could have diffused into the hydrogel and subsequently been released from the hydrogel, we believe that these proteins are likely not leading to the difference between the two substrates as they would be present in the serum during macrophage culture. Differences in the type and/or conformation of the adsorbed proteins are likely due to differences in material chemistry. Though hydrophobic surfaces are known to mediate protein unfolding, studies have reported that neutral hydrophilic surfaces can also induce protein unfolding [28,52]. Thus, it is possible that unfolded endogenous proteins interacting with PEG hydrogels may act as DAMPs, which subsequently induce an inflammatory response that is not observed on the reference substrate.

We have reported that proteins loosely adsorb on to PEG hydrogels [22] and thus it is reasonable to postulate that macrophages interact with the PEG surface through the layer of adsorbed proteins, the PEG surface itself, or both. Other studies have also reported leukocyte attachment on PEG-terminated self-assembled monolayers (SAMs) with pre-adsorbed plasma and interestingly attachment was higher than on methyl-terminated SAMs [53]. It is worth noting that macrophages express a range of integrins that facilitates their diverse functions *in vivo* [54]. As a result, macrophages have the ability to interact with proteins, such as albumin [55] to which many cell types (e.g., contractile adherent cells such as fibroblasts) lack integrins [56]. Moreover, we found that macrophages attach to the PEG hydrogel and TCPS without exogenous proteins, suggesting that macrophages have cell surface molecules capable of interacting with different material chemistries (e.g., hydrogen bonding with PEG or charge-charge interactions with TCPS). Although the exact mechanism remains to be determined, macrophage interactions with the PEG hydrogel or its adsorbed proteins up-regulated pro-inflammatory cytokine expression via MyD88-dependent

signaling. Other studies have reported that hydroxyl-terminated SAMs induced macrophage fusion to a greater extent than methyl-terminated or carboxylic acid-terminated SAMs [57], further suggesting the neutral, hydrophilic surfaces contribute to macrophage activation and fusion. Our *in vitro* findings also indicate the cytokines that are produced by a MyD88-independent pathway can lead to a feedback mechanism that initiates MyD88-dependent signaling, perhaps one that involves production and autocrine response to IL-1β. Overall these *in vitro* findings implicate cell-surface receptor recognition, that may include TLRs followed by subsequent IL-1β signaling, which leads to a hydrogel-induced inflammatory response.

In vivo, the temporal progression of the FBR to implanted biomaterials involves the initial recruitment of inflammatory cells. In WT mice, the presence of neutrophils and to a lesser extent monocytes on day 2 at the PEG hydrogel surface is consistent with an acute inflammatory response. Their persistent presence throughout the 28 d study is however indicative of a sustained and chronic inflammatory response. Due to the short lifespan of neutrophils, their presence in the FBR has traditionally been thought to be limited to the early stages of the FBR [58]. However, recent studies have shown that neutrophils are continuously recruited from circulation [59] and persist longer than previously thought. For example, neutrophils were present two weeks post implantation of alginate and poly(lactic acid-co-glycolic acid) microcapsules in the peritoneal cavity [18,60] and were present 30 days after delivery of titanium dioxide microparticles to the lung [61]. The FBR may therefore be indicative of a non-resolving inflammatory reaction [62], which is distinctly different from inflammation associated with wound healing or infection that eventually resolves. Macrophages were also present as early as 2 d. Peri-implant macrophages originate from blood monocytes or tissue-resident macrophage. We surmise that the initial infiltration of macrophages are tissue-resident macrophages, but at later times they are accompanied by monocytes that have differentiated into macrophages. Eosinophils were also detected at all time points, but at relatively low percentages (<4% of the total myeloid cell population); this is similar to reports that tissue-resident eosinophils comprise ~6% of the total myeloid cell population in naïve skin [63]. When MyD88 was mutated, the number of inflammatory cells accumulating at the implant surface was dramatically reduced. The relative ratios in myeloid subtypes also differed with far fewer neutrophils relative to monocytes and macrophages. The overall decrease in inflammatory cell numbers and the relative decrease in the percentage of neutrophils present during the FBR in MyD88$^{-/-}$ mice implicate MyD88 in the inflammatory response to implanted PEG hydrogels.

Most significantly, our data demonstrate that the fibrous capsule formation was largely mediated by MyD88. While this result is consistent with other studies investigating MyD88 in the development of fibrotic diseases including lung injury models [64,65], such a link has not previously been established in the FBR. Macrophages have been long implicated as the primary driver in fibrous encapsulation, and recent mouse studies confirmed that ablating all macrophages, but not neutrophils, prevents fibrous encapsulation [18]. In the MyD88$^{-/-}$ mice, the continual recruitment of neutrophils and monocytes suggest that other less potent inflammatory signals (e.g., via TRIF-signaling) may be sufficient to maintain an inflammatory response in the absence of MyD88 and drive fibrosis albeit at a much lower level.

While this study focused on the mechanisms that lead to the FBR to a singular PEG hydrogel, the FBR is considered a ubiquitous response. Studies have reported that a poly(ethylene oxide) coating applied to a fluorinated ethylene propylene copolymer induced a FBR similar to the copolymer without the coating [53]. However, a separate study reported that when polypropylene particles with different surface functionalities were implanted subcutaneously for two weeks, the implants led to a fibrous capsule, but the thickness of the capsule depended on the surface chemistry [66]. Notably, hydroxyl and amine surface chemistries led to a fibrous capsule that was thicker than methyl surface chemistries and carboxyl surface groups led to the thinnest capsule. This *in vivo* finding supports our *in vitro* results where the reference substrate of TCPS, which is decorated with carboxyl groups, exhibited lower macrophage activation when compared to the PEG hydrogels. Overall, the FBR reported herein to PEG hydrogels in WT mice is consistent with the FBR to other types of materials implanted subcutaneously. For example, poly(ether imide) films after 28 days implanted subcutaneously had positive staining for macrophages surrounding the implant and was encased in a fibrous capsule [67]. Poly(2-hydroxyethyl methacrylate) hydrogels led to the accumulation of a dense layer of inflammatory cells surrounded by a fibrous capsule after 21 days [68]. Crosslinked gelatin hydrogels also led to the accumulation of inflammatory cells at the implant surface and fibrous encapsulation after 21 days [69]. It is worth noting that although these studies confirmed the presence of macrophages by immunohistochemistry, the presence of neutrophils was not probed.

There are several limitations of this study. In the *in vitro* studies, culture medium containing serum proteins was used, and therefore, a direct substrate effect (i.e., PEG vs TCPS) was not determined. Instead, the macrophage response represents a combined substrate effect (i.e., chemistry and property) and substrate-induced effect (i.e., type and/or confirmation of surface adsorbed proteins). This study was limited to one formulation of PEG hydrogels and future research will need to investigate a broader spectrum of hydrogel stiffness and formulations to confirm MyD88-mediated fibrous encapsulation. We identified the presence of neutrophils by flow cytometry, but future studies will need to confirm their presence and location by immunohistochemistry. We were not able to identify foreign body giant cells at the hydrogel surface; the timing of the appearance of these cells has been correlated with the onset of the fibrous capsule [10]. Thus, the role of MyD88 in their formation remains to be determined. Finally, we chose to study stable PEG hydrogels in this study to minimize confounding factors with degradation. However, we previously reported that the FBR was similar to non-degradable PEG hydrogels and PEG hydrogels containing matrix-metalloproteinase sensitive crosslinks [70]. Despite these limitations, our results provide evidence that MyD88-inflammation drives the subsequent events that lead to fibrous encapsulation in response to implanted PEG hydrogels.

5. Conclusions

Our *in vitro* findings demonstrate the importance of MyD88 in the PEG hydrogel-mediated induction of pro-inflammatory cytokines. Moreover, the results *in vitro* indicate that recognition of material chemistry and/or the adsorbed proteins is responsible for macrophage activation and that this occurs primarily through MyD88-dependent signaling pathways, implicating TLRs followed by IL-1β signaling. The *in vivo* findings show that

MyD88 significantly contributes to neutrophil and macrophage accumulation and the subsequent events that lead to fibrous encapsulation to implanted synthetic hydrogels. Overall, this work provides evidence for the role of inflammation in mediating the FBR to PEG hydrogels and specifically the formation of the fibrous capsule by activating MyD88-dependent signaling. With a better understanding of the pathways underlying the FBR, our future work aims to design PEG hydrogels that can evade the FBR.

Supplementary Material

Refer to Web version on PubMed Central for supplementary material.

Acknowledgments

Research reported in this publication was supported by the National Institute of Arthritis and Musculoskeletal and Skin Diseases of the National Institute of Health and the National Institute of Allergy and Infectious Diseases under Award Numbers 1R21AR064436 and 1R21AI132827. The content is solely the responsibility of the authors and does not necessarily represent the official views of the National Institutes of Health. This work was also supported by the University of Colorado Innovative Seed Grant program and U.S. Department of Education GAANN fellowships to LDA and LSS.

References

[1]. Peppas NA, Hilt JZ, Khademhosseini A, Langer R, Hydrogels in biology and medicine: From molecular principles to bionanotechnology, Adv. Mater 18 (2006) 1345–1360. 10.1016/j.actamat.2012.10.046.

[2]. Spencer KC, Sy JC, Ramadi KB, Graybiel AM, Langer R, Cima MJ, Characterization of Mechanically Matched Hydrogel Coatings to Improve the Biocompatibility of Neural Implants., Sci. Rep 7 (2017) 1952. doi: 10.1038/s41598-017-02107-2 [PubMed: 28512291]

[3]. Boodagh P, Johnson R, Maly C, Ding Y, Tan W, Soft-sheath, stiff-core microfiber hydrogel for coating vascular implants., Colloids Surf. B Biointerfaces 183 (2019) 110395. doi:10.1016/j.colsurfb.2019.110395. [PubMed: 31386934]

[4]. Li D, Lv P, Fan L, Huang Y, Yang F, Mei X, Wu D, The immobilization of antibiotic-loaded polymeric coatings on osteoarticular Ti implants for the prevention of bone infections., Biomater. Sci 5 (2017) 2337–2346. doi:10.1039/c7bm00693d. [PubMed: 29034380]

[5]. McCall JD, Luoma JE, Anseth KS, Covalently tethered transforming growth factor beta in PEG hydrogels promotes chondrogenic differentiation of encapsulated human mesenchymal stem cells, Drug Deliv. Transl. Res 2 (2012) 305–312. doi:10.1007/s13346-012-0090-2. [PubMed: 23019539]

[6]. Raza A, Lin CC, The influence of matrix degradation and functionality on cell survival and morphogenesis in PEG-based hydrogels, Macromol. Biosci 13 (2013) 1048–1058. doi:10.1002/mabi.201300044. [PubMed: 23776086]

[7]. Van Hove AH, Burke K, Antonienko E, Brown E, Benoit DSW, Enzymatically-responsive pro-angiogenic peptide-releasing poly(ethylene glycol) hydrogels promote vascularization in vivo, J. Controlled Release 217 (2015) 191–201. doi:10.1016/j.jconrel.2015.09.005.

[8]. Lynn AD, Blakney AK, Kyriakides TR, Bryant SJ, Temporal progression of the host response to implanted poly(ethylene glycol)-based hydrogels., J. Biomed. Mater. Res. A 96 (2011) 621–31. doi:10.1002/jbm.a.33015. [PubMed: 21268236]

[9]. Ratner BD, Bryant SJ, Biomaterials: Where we have been and where we are going, Annu. Rev. Biomed. Eng 6 (2004) 41–75. doi: 10.1146/annurev.bioeng.6.040803.140027. [PubMed: 15255762]

[10]. Anderson JM, Rodriguez A, Chang DT, Foreign body reaction to biomaterials, Semin. Immunol 20 (2008) 86–100.doi: 10.1016/j.smim.2007.11.004. [PubMed: 18162407]

[11]. Helton KL, Ratner BD, Wisniewski NA, Biomechanics of the sensor-tissue interface-effects of motion, pressure, and design on sensor performance and the foreign body response-part I: theoretical framework., J. Diabetes Sci. Technol 5 (2011) 632–46. doi: 10.1177/193229681100500318. [PubMed: 21722578]

[12]. Swartzlander MD, Lynn AD, Blakney AK, Kyriakides TR, Bryant SJ, Understanding the host response to cell-laden poly(ethylene glycol)-based hydrogels., Biomaterials. 34 (2013) 952–64. doi:10.1016/j.biomaterials.2012.10.037. [PubMed: 23149012]

[13]. Saleh LS, Bryant SJ, The Host Response in Tissue Engineering: Crosstalk Between Immune cells and Cell-laden Scaffolds., Curr. Opin. Biomed. Eng 6 (2018) 58–65. doi:10.1016/j.cobme.2018.03.006. [PubMed: 30374467]

[14]. Lynn AD, Blakney AK, Kyriakides TR, Bryant SJ, Temporal progression of the host response to implanted poly(ethylene glycol) based hydrogels, J. Biomed. Mater. Res. A 96A (2011) 621–631. doi: 10.1002/jbm.a.33015.

[15]. Suggs LJ, Krishnan RS, Garcia CA, Peter SJ, Anderson JM, Mikos AG, In vitro and in vivo degradation of poly(propylene fumarate-co-ethylene glycol) hydrogels, J. Biomed. Mater. Res 42 (1998) 312–320. doi: 10.1002/(sici)1097-4636(199811)42:2<312::aid-jbm17>3.0.co;2-k. [PubMed: 9773828]

[16]. Luttikhuizen DT, Harmsen MC, Van Luyn MJA, Cellular and molecular dynamics in the foreign body reaction, Tissue Eng. 12 (2006) 1955–1970. doi: 10.1089/ten.2006.12.1955. [PubMed: 16889525]

[17]. Anderson JM, McNally AK, Biocompatibility of implants: lymphocyte/macrophage interactions, Semin. Immunopathol 33 (2011) 221–233. doi: 10.1007/s00281-011-0244-1. [PubMed: 21271251]

[18]. Doloff JC, Veiseh O, Vegas AJ, Tam HH, Farah S, Ma M, Li J, Bader A, Chiu A, Sadraei A, Aresta-Dasilva S, Griffin M, Jhunjhunwala S, Webber M, Siebert S, Tang K, Chen M, Langan E, Dholokia N, Thakrar R, Qi M, Oberholzer J, Greiner DL, Langer R, Anderson DG, Colony stimulating factor-1 receptor is a central component of the foreign body response to biomaterial implants in rodents and non-human primates., Nat. Mater 16 (2017) 671–680. doi:10.1038/nmat4866. [PubMed: 28319612]

[19]. Takeda K, Akira S, TLR signaling pathways, Semin. Immunol 16 (2004) 3–9. doi:10.1016/j.smim.2003.10.003. [PubMed: 14751757]

[20]. Liu Y, Yin H, Zhao M, Lu Q, TLR2 and TLR4 in Autoimmune Diseases: a Comprehensive Review, Clin. Rev. Allergy Immunol 47 (2014) 136–147. doi:10.1007/s12016-013-8402-y. [PubMed: 24352680]

[21]. Crisan TO, Netea MG, Joosten LAB, Innate immune memory: Implications for host responses to damage-associated molecular patterns, Eur. J. Immunol 46 (2016) 817–828. doi:10.1002/eji.201545497. [PubMed: 26970440]

[22]. Swartzlander MD, Bryant SJ, Linking the foreign body response and protein adsorption to PEG-based hydrogels using proteomics, Biomaterials. 41 (2015) 26–36. doi:10.1016/j.biomaterials.2014.11.026. [PubMed: 25522962]

[23]. Yu L, Wang LT, Chen SW, Endogenous toll-like receptor ligands and their biological significance, J. Cell. Mol. Med 14 (2010) 2592–2603. doi:10.1111/j.1582-4934.2010.01127.x. [PubMed: 20629986]

[24]. Vabulas RM, Ahmad-Nejad P, Ghose S, Kirschning CJ, Issels RD, Wagner H, HSP70 as endogenous stimulus of the toll/interleukin-1 receptor signal pathway, J. Biol. Chem 277 (2002) 15107–15112. doi:10.1074/jbc.M111204200. [PubMed: 11842086]

[25]. Asea A, Rehli M, Kabingu E, Boch JA, Bare O, Auron PE, Stevenson MA, Calderwood SK, Novel signal transduction pathway utilized by extracellular HSP70 - Role of Toll-like receptor (TLR) 2 AND TLR4, J. Biol. Chem 277 (2002) 15028–15034. doi:10.1074/jbc.M200497200. [PubMed: 11836257]

[26]. Okamura Y, Watari M, Jerud ES, Young DW, Ishizaka ST, Rose J, Chow JC, J.F. 3rd Strauss, The extra domain A of fibronectin activates Toll-like receptor 4., J. Biol. Chem 276 (2001) 10229–10233. doi:10.1074/jbc.M100099200. [PubMed: 11150311]

[27]. Smiley ST, King JA, Hancock WW, Fibrinogen stimulates macrophage chemokine secretion through toll-like receptor 4., J. Immunol. Baltim. Md 1950 167 (2001) 2887–2894. doi: 10.4049/jimmunol.167.5.2887.

[28]. McLoughlin SY, Kastantin M, Schwartz DK, Kaar JL, Single-molecule resolution of protein structure and interfacial dynamics on biomaterial surfaces, Proc Natl Acad Sci U A 110 (2013) 19396–19401. doi:10.1073/pnas.1311761110.

[29]. Swartzlander MD, Barnes CA, Blakney AK, Kaar JL, Kyriakides TR, Bryant SJ, Linking the foreign body response and protein adsorption to PEG-based hydrogels using proteomics, Biomaterials. 41 (2015) 26–36. doi:10.1016/j.biomaterials.2014.11.026. [PubMed: 25522962]

[30]. Seong SY, Matzinger P, Hydrophobicity: an ancient damage-associated molecular pattern that initiates innate immune responses, Nat. Rev. Immunol 4 (2004) 469–478. doi:10.1038/nri1372. [PubMed: 15173835]

[31]. Krysko DV, Garg AD, Kaczmarek A, Krysko O, Agostinis P, Vandenabeele P, Immunogenic cell death and DAMPs in cancer therapy, Nat. Rev. Cancer 12 (2012) 860–875. doi:10.1038/nrc3380. [PubMed: 23151605]

[32]. Land WG, The Role of Damage-Associated Molecular Patterns (DAMPs) in Human Diseases: Part II: DAMPs as diagnostics, prognostics and therapeutics in clinical medicine., Sultan Qaboos Univ. Med. J 15 (2015) e157–170. [PubMed: 26052447]

[33]. Keselowsky BG, Bridges AW, Burns KL, Tate CC, Babensee JE, LaPlaca MC, Garcia AJ, Role of plasma fibronectin in the foreign body response to biomaterials, Biomaterials. 28 (2007) 3626–3631. doi:10.1016/j.biomaterials.2007.04.035. [PubMed: 17521718]

[34]. Mckiel L, Fitzpatrick L, Damage-associated molecular patterns in the adsorbed protein layer on biomaterial surfaces, Frontiers in Bioengineering and Biotechnology (n.d.). doi:10.3389/conf.FBIOE.2016.01.01515.

[35]. Rogers TH, Babensee JE, Altered adherent leukocyte profile on biomaterials in Toll-like receptor 4 deficient mice, Biomaterials. 31 (2010) 594–601. doi:10.1016/j.biomaterials.2009.09.077. [PubMed: 19818491]

[36]. Auquit-Auckbur I, Caillot F, Arnoult C, Menard J-F, Drouot L, Courville P, Tron F, Musette P, Role of Toll-like receptor 4 in the inflammation reaction surrounding silicone prosthesis, Acta Biomater. 7 (2011) 2047–2052. doi:10.1016/j.actbio.2011.01.030. [PubMed: 21272673]

[37]. Deguine J, Barton GM, MyD88: a central player in innate immune signaling., F1000prime Rep. 6 (2014) 97–97. doi:10.12703/P6-97. [PubMed: 25580251]

[38]. Kawai T, Adachi O, Ogawa T, Takeda K, Akira S, Unresponsiveness of MyD88-deficient mice to endotoxin, Immunity. 11 (1999) 115–22. doi: 10.1016/s1074-7613(00)80086-2. [PubMed: 10435584]

[39]. Takeuchi O, Hoshino K, Akira S, Cutting edge: TLR2-deficient and MyD88-deficient mice are highly susceptible to Staphylococcus aureus infection., J. Immunol. Baltim. Md 1950 165 (2000) 5392–5396. doi: 10.4049/jimmunol.165.10.5392.

[40]. Liang MD, Bagchi A, Warren HS, Tehan MM, Trigilio JA, Beasley-Topliffe LK, Tesini BL, Lazzaroni JC, Fenton MJ, Hellman J, Bacterial peptidoglycan-associated lipoprotein: A naturally occurring toll-like receptor 2 agonist that is shed into serum and has synergy with lipopolysaccharide, J. Infect. Dis 191 (2005) 939–948. doi:10.1086/427815. [PubMed: 15717270]

[41]. Pearl JI, Ma T, Irani AR, Huang Z, Robinson WH, Smith RL, Goodman SB, Role of the Toll-like receptor pathway in the recognition of orthopedic implant wear-debris particles, Biomaterials. 32 (2011) 5535–5542. doi:10.1016/j.biomaterials.2011.04.046. [PubMed: 21592562]

[42]. Shokouhi B, Coban C, Hasirci V, Aydin E, Dhanasingh A, Shi N, Koyama S, Akira S, Zenke M, Sechi AS, The role of multiple toll-like receptor signalling cascades on interactions between biomedical polymers and dendritic cells, Biomaterials. 31 (2010) 5759–5771. doi:10.1016/j.biomaterials.2010.04.015. [PubMed: 20452017]

[43]. Paredes-Juarez GA, de Haan BJ, Faas MM, de Vos P, The role of pathogen-associated molecular patterns in inflammatory responses against alginate based microcapsules, J. Controlled Release. 172 (2013) 983–992. doi:10.1016/j.jconrel.2013.09.009.

[44]. Lynn AD, Kyriakides TR, Bryant SJ, Characterization of the in vitro macrophage response and in vivo host response to poly(ethylene glycol)-based hydrogels, J. Biomed. Mater. Res. A 93A (2010) 941–953. doi:10.1002/jbm.a.32595.

[45]. Lynn AD, Bryant SJ, Phenotypic changes in bone marrow-derived murine macrophages cultured on PEG-based hydrogels activated or not by lipopolysaccharide, Acta Biomater. 7 (2011) 123–132. doi:10.1016/j.actbio.2010.07.033. [PubMed: 20674808]

[46]. Jay SM, Skokos E, Laiwalla F, Krady M-M, Kyriakides TR, Foreign body giant cell formation is preceded by lamellipodia formation and can be attenuated by inhibition of Rac1 activation., Am. J. Pathol 171 (2007) 632–640. doi:10.2353/ajpath.2007.061213. [PubMed: 17556592]

[47]. Pfaffl MW, A new mathematical model for relative quantification in real-time RT-PCR., Nucleic Acids Res. 29 (2001) e45. doi: 10.1093/nar/29.9.e45. [PubMed: 11328886]

[48]. Weber LM, Lopez CG, Anseth KS, Effects of PEG hydrogel crosslinking density on protein diffusion and encapsulated islet survival and function, J. Biomed. Mater. Res. A 90A (2009) 720–729. doi:10.1002/jbm.a.32134.

[49]. Badylak SF, Valentin JE, Ravindra AK, McCabe GP, Stewart-Akers AM, Macrophage phenotype as a determinant of biologic scaffold remodeling., Tissue Eng. Part A 14 (2008) 1835–42. doi: 10.1089/ten.tea.2007.0264. [PubMed: 18950271]

[50]. Vogler EA, Structure and reactivity of water at biomaterial surfaces, Adv Colloid Interface Sci. 74 (1998) 69–117. doi: 10.1016/S0001-8686(97)00040-7. [PubMed: 9561719]

[51]. Francis GL, Albumin and mammalian cell culture: implications for biotechnology applications, Cytotechnology. 62 (2010) 1–16. doi:10.1007/s10616-010-9263-3. [PubMed: 20373019]

[52]. Sivaraman B, Latour RA, The relationship between platelet adhesion on surfaces and the structure versus the amount of adsorbed fibrinogen, Biomaterials. 31 (2010) 832–839. doi: 10.1016/j.biomaterials.2009.10.008. [PubMed: 19850334]

[53]. Shen MC, Martinson L, Wagner MS, Castner DG, Ratner BD, Horbett TA, PEO-like plasma polymerized tetraglyme surface interactions with leukocytes and proteins: in vitro and in vivo studies, J. Biomater. Sci.-Polym. Ed 13 (2002) 367–390. doi: 10.1163/156856202320253910. [PubMed: 12160299]

[54]. Brown EJ, Integrins of Macrophages and Macrophage-Like Cells, in: Gordon S (Ed.), Macrophage Ther. Target, Springer Berlin Heidelberg, Berlin, Heidelberg, 2003: pp. 111–130. doi:10.1007/978-3-642-55742-2_7.

[55]. Brevig T, Holst B, Ademovic Z, Rozlosnik N, Rohrmann JH, Larsen NB, Hansen OC, Kingshott P, The recognition of adsorbed and denatured proteins of different topographies by beta2 integrins and effects on leukocyte adhesion and activation., Biomaterials. 26 (2005) 3039–3053. doi:10.1016/j.biomaterials.2004.09.006. [PubMed: 15603799]

[56]. Grinnell F, Feld MK, Initial adhesion of human fibroblasts in serum-free medium: possible role of secreted fibronectin., Cell. 17 (1979) 117–129. doi:10.1016/0092-8674(79)90300-3. [PubMed: 378401]

[57]. Jones JA, Qin LA, Meyerson H, Kwon IK, Matsuda T, Anderson JM, Instability of self-assembled monolayers as a model material system for macrophage/FBGC cellular behavior, J. Biomed. Mater. Res. A 86A (2008) 261–268. doi:10.1002/jbm.a.31660.

[58]. Anderson JM, Biological responses to materials, Annu. Rev. Mater. Res 31 (2001) 81–110. doi: 10.1146/annurev.matsci.31.1.81.

[59]. Jhunjhunwala S, Alvarez D, Aresta-DaSilva S, Tang K, Tang BC, Greiner DL, Newburger PE, von Andrian UH, Langer R, Anderson DG, Frontline Science: Splenic progenitors aid in maintaining high neutrophil numbers at sites of sterile chronic inflammation., J. Leukoc. Biol 100 (2016) 253–260. doi:10.1189/jlb.1HI0615-248RR. [PubMed: 26965635]

[60]. Jhunjhunwala S, Aresta-DaSilva S, Tang K, Alvarez D, Webber MJ, Tang BC, Lavin DM, Veiseh O, Doloff JC, Bose S, Vegas A, Ma M, Sahay G, Chiu A, Bader A, Langan E, Siebert S, Li J, Greiner DL, Newburger PE, von Andrian UH, Langer R, Anderson DG, Neutrophil Responses to Sterile Implant Materials., PloS One. 10 (2015) e0137550. doi:10.1371/journal.pone.0137550. [PubMed: 26355958]

[61]. Gustafsson A, Lindstedt E, Elfsmark LS, Bucht A, Lung exposure of titanium dioxide nanoparticles induces innate immune activation and long-lasting lymphocyte response in the

Dark Agouti rat., J. Immunotoxicol 8 (2011) 111–121. doi:10.3109/1547691X.2010.546382. [PubMed: 21309687]

[62]. Nathan C, Ding A, Nonresolving Inflammation, Cell. 140 (2010) 871–882. doi:10.1016/j.cell.2010.02.029. [PubMed: 20303877]

[63]. Weller PF, Spencer LA, Functions of tissue-resident eosinophils., Nat. Rev. Immunol 17 (2017) 746–760. doi:10.1038/nri.2017.95. [PubMed: 28891557]

[64]. Re SL, Giordano G, Yakoub Y, Devosse R, Uwambayinema F, Couillin I, Ryffel B, Marbaix E, Lison D, Huaux F, Uncoupling between inflammatory and fibrotic responses to silica: evidence from MyD88 knockout mice., PloS One. 9 (2014) e99383. doi:10.1371/journal.pone.0099383. [PubMed: 25050810]

[65]. Gasse P, Mary C, Guenon I, Noulin N, Charron S, Schnyder-Candrian S, Schnyder B, Akira S, Quesniaux VFJ, Lagente V, Ryffel B, Couillin I, IL-1R1/MyD88 signaling and the inflammasome are essential in pulmonary inflammation and fibrosis in mice., J. Clin. Invest 117 (2007) 3786–3799. doi:10.1172/JCI32285. [PubMed: 17992263]

[66]. Kamath S, Bhattacharyya D, Padukudru C, Timmons RB, Tang L, Surface chemistry influences implant-mediated host tissue responses, J. Biomed. Mater. Res. A 86A (2008) 617–626. doi:10.1002/jbm.a.31649.

[67]. Haase T, Krost A, Sauter T, Kratz K, Peter J, Kamann S, Jung F, Lendlein A, Zohlnhoefer D, Rueder C, In vivo biocompatibility assessment of poly (ether imide) electrospun scaffolds, J. Tissue Eng. Regen. Med 11 (2017) 1034–1044. doi:10.1002/term.2002. [PubMed: 25712330]

[68]. Sussman EM, Halpin MC, Muster J, Moon RT, Ratner BD, Porous Implants Modulate Healing and Induce Shifts in Local Macrophage Polarization in the Foreign Body Reaction, Ann. Biomed. Eng 42 (2014) 1508–1516. doi:10.1007/s10439-013-0933-0. [PubMed: 24248559]

[69]. Yu T, Wang W, Nassiri S, Kwan T, Dang C, Liu W, Spiller KL, Temporal and spatial distribution of macrophage phenotype markers in the foreign body response to glutaraldehyde-crosslinked gelatin hydrogels, J.Biomater. Sci.-Polym. Ed 27 (2016) 721–742. doi:10.1080/09205063.2016.1155881. [PubMed: 26902292]

[70]. Amer LD, Bryant SJ, The In Vitro and In Vivo Response to MMP-Sensitive Poly(Ethylene Glycol) Hydrogels., Ann. Biomed. Eng 44 (2016) 1959–1969. doi:10.1007/s10439-016-1608-4. [PubMed: 27080375]

Statement of Significance

Synthetic hydrogels are promising for *in vivo* applications but, like all non-biological biomaterials, synthetic hydrogels elicit a foreign body response (FBR). The molecular mechanisms that drive the FBR are not well understood. This work identifies the myeloid differentiation primary response gene 88 (MyD88) as a central mediator to macrophage activation in response to a poly(ethylene glycol) hydrogel with pre-adsorbed proteins *in vitro*. Moreover, MyD88 was also central to the recruitment of inflammatory cells, which included neutrophils, monocytes, and macrophages, to implanted PEG hydrogels and to fibrous encapsulation. These findings demonstrate that MyD88-mediated inflammation is responsible in part for the formation of the fibrous capsule of the FBR.

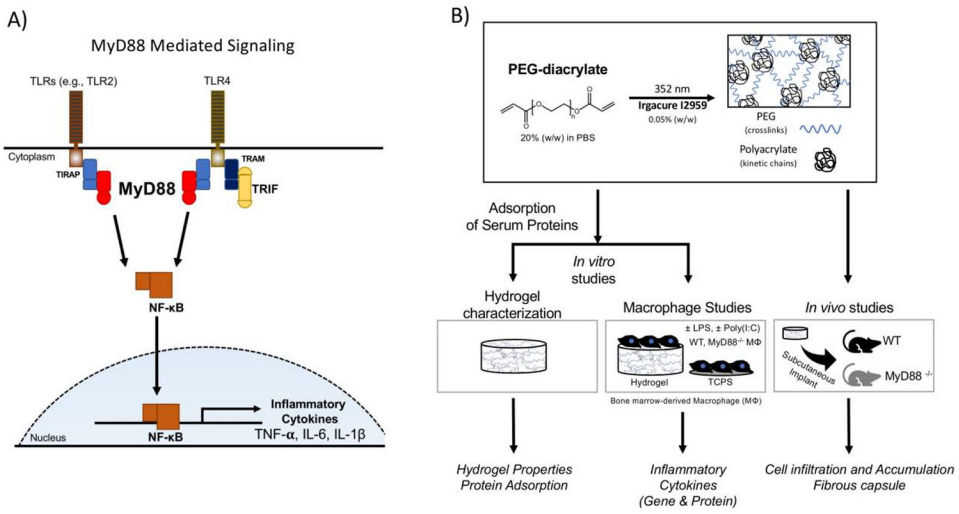

Fig. 1.

A) MyD88-mediated signaling induced by TLRs lead to NF-κB transcription of proinflammatory cytokines. Host proteins acting as damage-associated molecular patterns (DAMPs) such as unfolded proteins can bind to TLRs (e.g., TLR 2 and TLR4) to induce MyD88-mediated signaling. B) Experimental set-up: PEG hydrogels were formed from PEG diacrylate macromers by photopolymerization to form hydrogels that have polyacrylate kinetic chains crosslinked with PEG chains. Experimental approach for *in vitro* studies consisted of characterization of hydrogel properties and protein adsorption and activation of bone-marrow macrophages derived from wildtype (WT) or MyD88$_{-/-}$ mice. Experimental approach for *in vivo* studies consisted of characterization of PEG hydrogels that were implanted subcutaneously in WT or MyD88$_{-/-}$ mice.

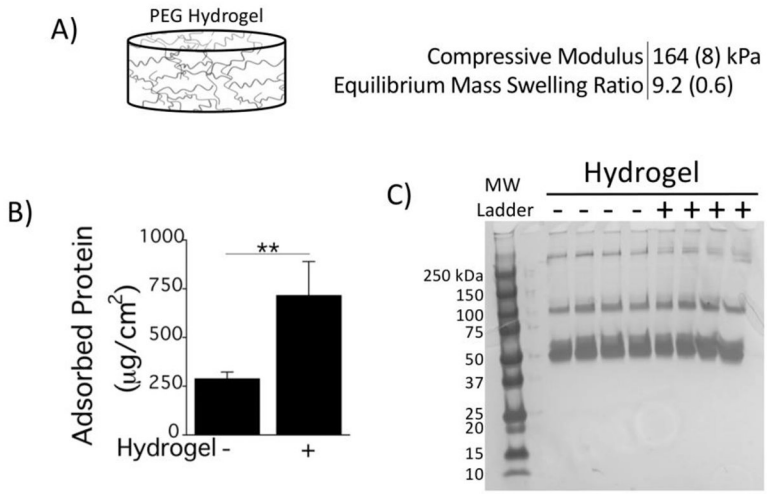

Fig. 2.

A) Properties of the PEG Hydrogel used in this study. B) Total amount of adsorbed protein following a 2 h incubation in fetal bovine serum for PEG hydrogels and the reference substrate (tissue culture polystyrene, TCPS). C) Protein signature of adsorbed proteins on PEG hydrogels (+Hydrogel) and the reference substrate (−Hydrogel) via silver stained SDS-PAGE are shown for four replicates of each condition along with a molecular weight (MW) ladder standard. MWs of each band in the ladder are denoted to the left of the protein gel. Data are presented as mean with standard deviation as error bars (n=4) and with *p*-values from pairwise comparisons (** $p<0.01$).

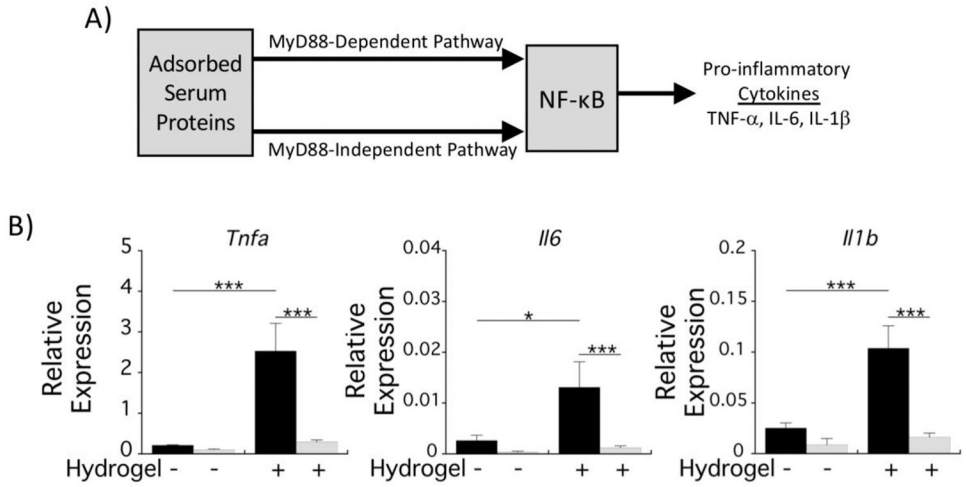

Fig. 3.

Macrophage activation on PEG hydrogels is mediated by MyD88. A) Schematic of MyD88-dependent and MyD88-independent signaling by pre-adsorbed proteins. B) mRNA production of the pro-inflammatory cytokine genes *Tnfa*, *Il6*, and *Il1b* relative to the housekeeping gene, *Rpl32* for WT (black bars) and MyD88$_{-/-}$ (gray bars) macrophages 4 h postseeding.

Data are presented as mean with standard deviation as error bars (n=4) and with *p*values from pairwise comparisons (* $p<0.05$; *** $p<0.001$).

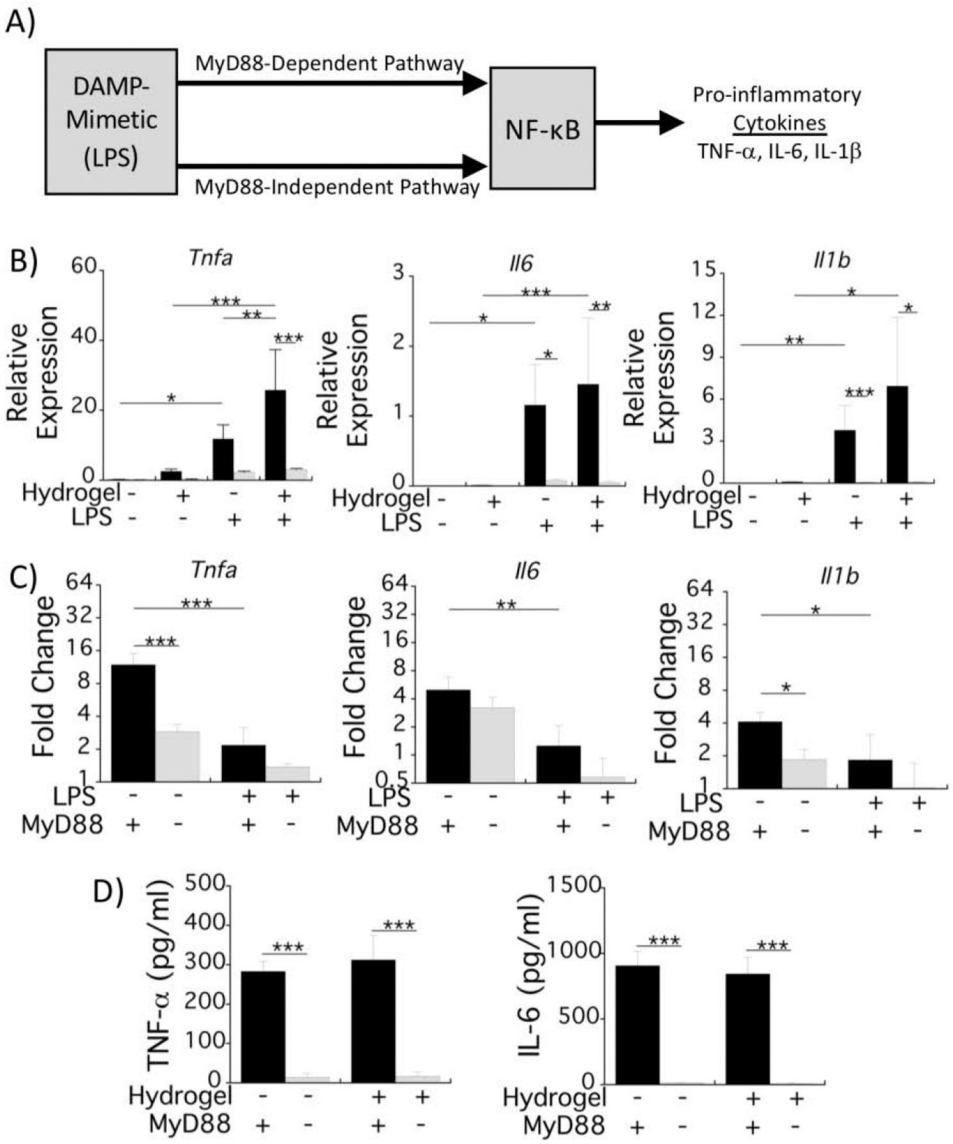

Fig. 4.

Macrophage activation on PEG hydrogels induced by the DAMP-mimetic, LPS, is mediated by MyD88. A) Schematic depicting the LPS-induced signaling for NF-κB via MyD88-dependent and MyD88-independent up-regulation of pro-inflammatory cytokines. Experimental setup is similar to Fig. 1A, but with the addition of LPS. B) mRNA expression of the proinflammatory cytokines, *Tnfa*, *Il6*, and *Il1b*, relative to the housekeeping gene, *Rpl32* for WT (black bars) and MyD88$_{-/-}$ (gray bars) macrophages with and without LPS stimulation. The unstimulated condition is the same data in Fig. 1C,D) Hydrogel-induced fold change in mRNA production for each cytokine is represented by relative mRNA production on the hydrogel condition normalized to that on the reference substrate for WT (black bars) and MyD88$_{-/-}$ (gray bars) macrophages. For both B&C panels, mRNA expression was analyzed 4 h after the exposures were started. D) Pro-inflammatory cytokine protein concentrations in the culture medium for WT (black bars) and MyD88$_{-/-}$ (gray bars)

macrophages with LPS stimulation after 24 h. All data are presented as mean with standard deviation as error bars (n=4) and with *p*values from pairwise comparisons (* $p<0.05$, ** $p<0.01$, and *** $p<0.001$).

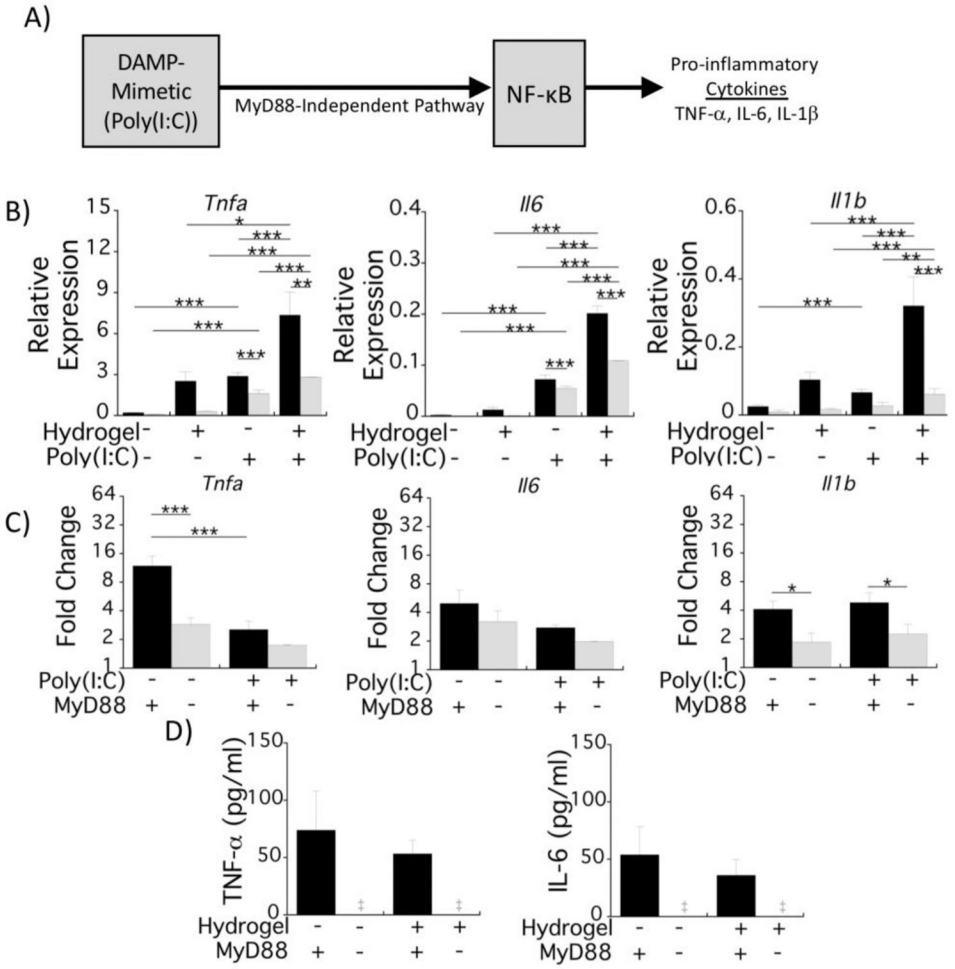

Fig. 5.

Macrophage activation on PEG hydrogels induced by the DAMP-mimetic, Poly(I:C), is moderately mediated by MyD88. A) Schematic depicting poly(I:C)-induced signaling for NF-κB via MyD88-independent up-regulation of pro-inflammatory cytokines. Experimental setup is similar to Fig. 1A, but with the addition of poly(I:C). B) mRNA production of the proinflammatory cytokines *Tnfa*, *Il6*, and *Il1b* relative to the housekeeping gene *Rpl32* for WT (black bars) and MyD88$_{-/-}$ (gray bars) macrophages in response to stimulation with poly(I:C). The unstimulated condition is the same data in Fig. 1D,C) Hydrogel-induced fold change in mRNA production for each cytokine is represented by relative mRNA production on the hydrogel condition normalized to that on the reference substrate for WT (black bars) and MyD88$_{-/-}$ (gray bars) macrophages. For both B&C panels, mRNA expression was analyzed 4 h post-seeding. D) Pro-inflammatory cytokine concentrations in the culture medium for WT (black bars) and MyD88$_{-/-}$ (gray bars) macrophages with LPS stimulation after 24 h. All data are presented as mean with standard deviation as error bars (n=4) with *P*-values shown for pairwise comparisons (* $p<0.05$; ** $p<0.01$; *** $p<0.001$).

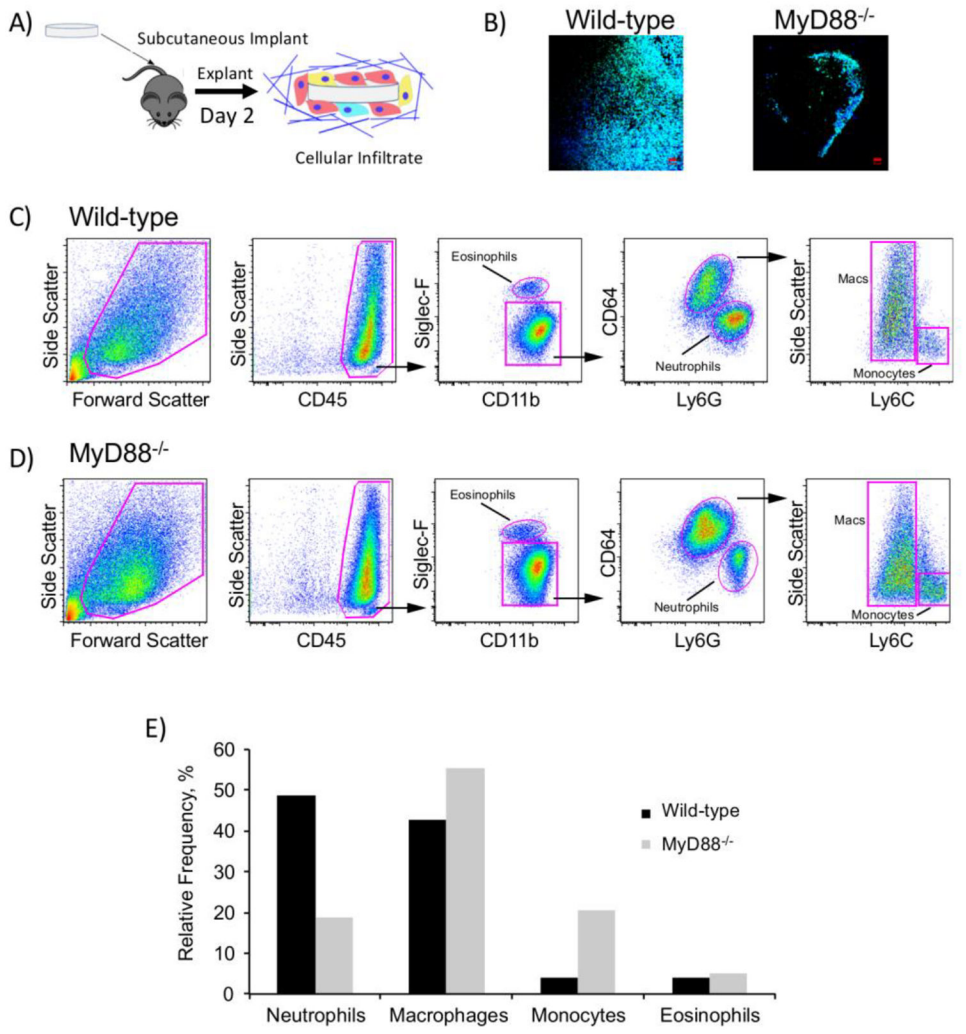

Fig. 6.

In vivo assessment of the FBR and the cells that interrogate the implant surface at 2 d. A) Schematic depicting implantation and subsequent analysis. B) Representative confocal microscopy images of hydrogels explanted after 2 d showing cell attachment to the surface. Cells were strained with F-actin (green) and counterstained with DAPI for cell nuclei (blue); scale bar is 50 μm. C, D) Flow cytometry assessment of leukocytes in and around the implant after 2 d. Hydrogels and surrounding tissue were explanted and enzymatically digested. Cell suspensions were stained with monoclonal antibodies and leukocytes assessed with flow cytometry. Four hydrogel implants were pooled to achieve sufficient cell numbers to perform flow cytometry. Gating strategies and representative dot plots are shown for WT (C) and MyD88$_{-/-}$ mice (D). E) Relative frequency of each leukocyte subset.

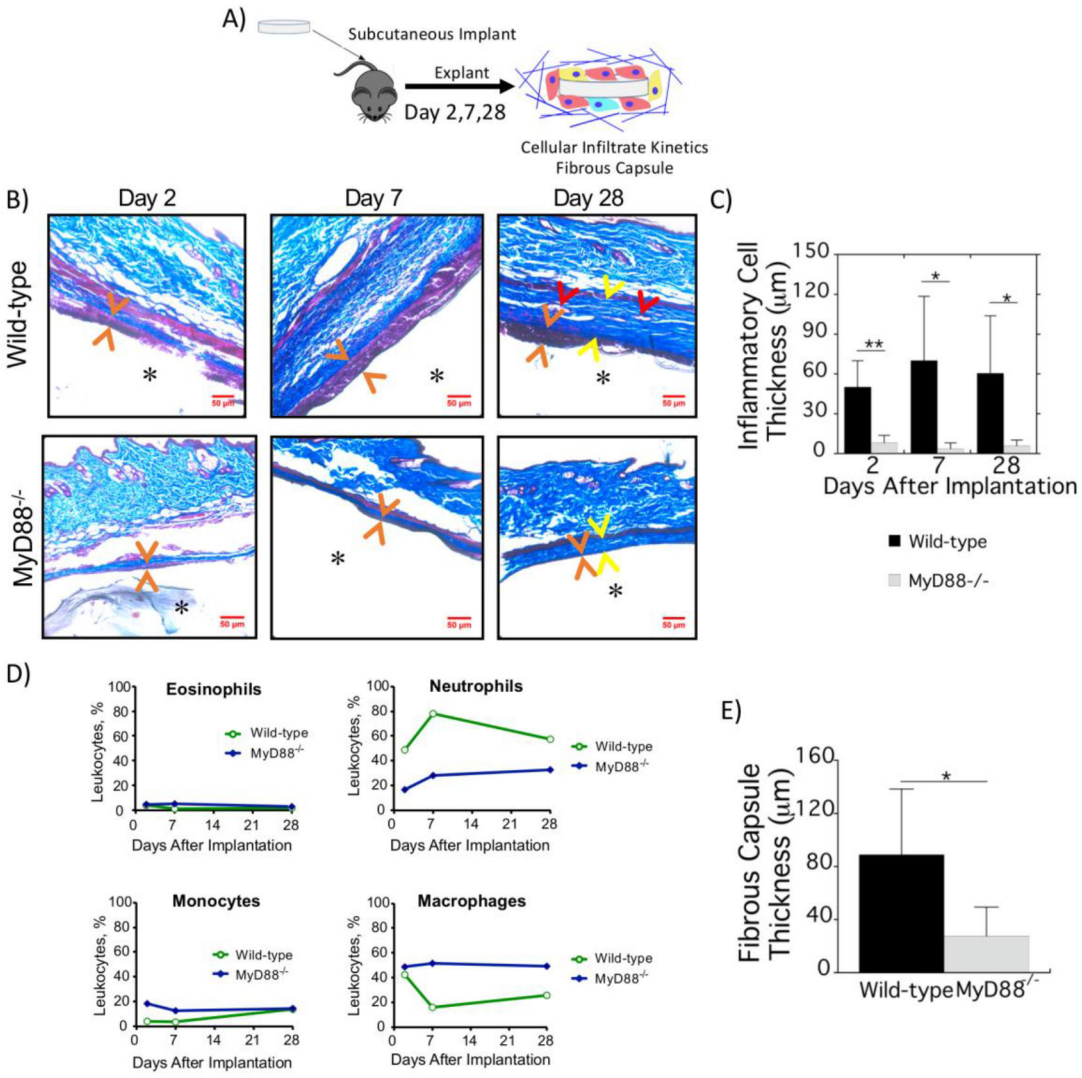

Fig. 7.

Inflammation and fibrosis of the FBR to implanted synthetic hydrogels is mediated by MyD88. A) Schematic depicting implantation and subsequent analysis. B) Hydrogels explanted after 2, 7, and 28 d from WT (top) and MyD88$_{-/-}$ (bottom) mice were stained with Masson's Trichrome. Orange arrows indicate the location of inflammatory cells at the surface of the hydrogels. At 28 d, yellow arrows indicate the fibrous capsule and red arrows indicate blood vessels. C) Quantification of the inflammatory cell thickness at the surface of implanted hydrogels at 2, 7 and 28 d in WT (black bars) and MyD88$_{-/-}$ (gray bars) mice. D) Relative percentages of inflammatory cells surrounding implants in WT and MyD88$_{-/-}$ mice from four hydrogel implants that were pooled to achieve sufficient cell numbers to perform flow cytometry. E) Quantification of the fibrous capsule thickness surrounding implants at 28 d in WT (black bars) and MyD88$_{-/-}$ (gray bars) mice. Data are presented as mean with standard deviation as error bars (n=4–8) with * $p<0.05$ and ** $p<0.01$.

Table 1 -

Primer Sequences used for qRT-PCR

Gene of Interest	Primer Sequence	Efficiency
Rpl32	F: CCATCTGTTTTACGGCATCATG	2.12
	R: TGAACTTCTTGGTCCTCTTTTTGA	
Tnfa	F: CACCGTCAGCCGATTTGC	1.99
	R: TTGACGGCAGAGAGGAGGTT	
Il6	F: T CGGAGGCTTAATTACACAT GTTC	2.00
	R: TGCCATTGCACAACTCTTTTCT	
Illb	F: CAGGTCGCTCAGGGTCACA	2.06
	R: TCAGAGGCAAGGAGGAAAACA	